ELSEVIER

Salt effects in capillary zone electrophoresis
III. Systematic and selective factors in the high ionic strength separation of sulphonamides in sodium phosphate buffers

Reginald F. Cross*, Jing Cao

School of Engineering and Science, Swinburne University of Technology, John Street, Hawthorn, Victoria 3122, Australia

Abstract

The effect of high concentrations of sodium phosphate buffer (65–210 mM) on the capillary zone electrophoretic separation of 23 sulphonamides and the neutral marker have been examined at pH 7 and 18 kV. In 65 mM phosphate, all ionised analytes (21 of the 23 sulphonamides) are resolved sufficiently for screening purposes. At higher buffer concentrations, general resolution clearly improves due to the systematic salt effect, which provides increased separation space. This effect is progressively enhanced by Joule heating via increases in the electrophoretic mobilities of the analytes migrating away from the detector. However, one pair of analytes displays unfavourable selectivity changes and comigrates at higher buffer concentrations. This has been demonstrated to be due to selective but dissimilar salt effects upon the degrees of ionisation of the two analytes that leads to a convergence of their electrophoretic mobilities. Eighteen sulphonamides were baseline-resolved between 174 and 210 mM sodium phosphate buffer. © 1998 Elsevier Science B.V. All rights reserved.

Keywords: Salt effects; Buffer composition; Sulphonamides

1. Introduction

The separation of sulphonamides (SFAs) by instrumental techniques has previously been reviewed [1,2]. In the latter case, the first data was presented for capillary zone electrophoretic (CZE) screening of a large number of the SFAs. That study showed a general increase in the apparent migration times (t_{app}) of the SFAs as the (phosphate) buffer concentration increased. As Janini et al. [3] have pointed out, this appears to be a general phenomenon. Wieme [4] has suggested an inverse proportionality between

the electrophoretic mobility (μ_{ep}) and the square root of the ionic strength of the buffer ($\sqrt{I}$). We have recently shown [5] that this relationship can be simply derived if the thickness of the electrical double layer is set equal to the "inverse Debye–Huckel" length. Janini et al. [3] have taken the simplest case (of a 1:1 electrolyte) and thus arrived at $\mu_{ep} \propto 1/\sqrt{C}$, where C is the concentration of the buffer. They also argued that the electroosmotic mobility (μ_{eo}) should be similarly affected. As they conclude, this leads to direct proportionality between t_{app} and $\sqrt{C}$. Their experimental data for the dansyl derivatives of amino acids and a neutral marker clearly demonstrate all of the above. The linearity of

---

*Corresponding author.

these t_{app} versus $\sqrt{C}$ plots was from 0.025 M up to the highest concentrations examined (0.075 M) in both of the buffers examined (acetate at pH 5 and phosphate at pH 7). As $C \propto I$, all of the theory [3–5] and experimental results [3] are entirely consistent.

Overall, the clear implication of the above relationships is increasing resolution with salt concentration and Janini et al. [3] have analysed their results to show this. However, the linearity of the relationship between t_{app} and $\sqrt{I}$ presumes a simple progression of physico–chemical effects (upon μ_{ep} and μ_{eo}) and the absence of the introduction of secondary effects which also depend upon C.

At fixed voltage, increasing C will lead to the onset and increasing effects of Joule heating due to the decreased Ohmic resistance of the solution [6]. On the other hand, this departure from linearity will not prevent further increases in resolution with further increases in C. Indeed the trend to improved resolution should continue, albeit at a changed rate. Exactly this phenomenon has been observed in a study of the CZE separation of dihydrofolate reductase inhibitors (DHFRIs) [7,8]. After pH optimisation, the most difficult to separate pair were only resolved in 0.25 M phosphate. In the high range of buffer concentrations (0.09–0.25 M), plots of t_{app} versus $\sqrt{C}$ strongly curved over [8], thus indicating the possible onset of Joule heating. However, the advantage of heightened separation was achieved without the attendant loss of efficiency which would be expected to arise eventually if the salt concentration was increased too far.

For partly ionised analytes, the differently charged acid and base conjugates will be subject to differential salt effects upon their activities and changes in ionisation will occur [6]. In this case the relativities of migrating species will alter and the gain or loss in selectivity will be determined by the initial relativity, by which analyte it is in any pair that deviates from the simple progression of t_{app} with increasing I, and, by the direction of the deviation.

This paper presents data obtained from an investigation of the CZE separation of 23 SFAs as a function of salt concentration at high phosphate levels. In view of the difficult DHFRI separation being achieved in sodium phosphate [7], we again chose the sodium salt. In conjunction with determinations of the changing ionisation states of analytes

displaying selective behaviour, a detailed analysis of the mechanisms of mobility modification is given for the changes in the separation that occur with increasing buffer concentration.

2. Theory

The apparent mobility (μ_{app}) and migration time (t_{app}) are related by Eq. (1):

$$t_{app} = \frac{L_D L}{V \mu_{app}} \tag{1}$$

where L_D is the distance to the detector, L is the distance between the electrodes and V is the applied voltage. Hence for conventional CZE of negatively charged analytes migrating away from the detector and in the opposite direction to the electroosmotic flow (EOF), Eq. (1) yields:

$$t_{app} = a \frac{1}{\mu_{eo} - \mu_{ep}} \tag{2}$$

where μ_{eo} is the electroosmotic mobility, μ_{ep} is the electrophoretic mobility and $a = L_D L / V$ (which will be constant if V is fixed). Thus for two analytes j and i:

$$\Delta t_{app} = a \left\{ \left(\frac{1}{\mu_{eo} - \mu_{ep}^{(j)}} \right) - \left(\frac{1}{\mu_{eo} - \mu_{ep}^{(i)}} \right) \right\} \tag{3}$$

Assuming the inverse dependences of μ_{eo} and μ_{ep} upon $\sqrt{I}$ [3–5,9]:

$$\Delta t_{app} = a \left\{ \left[\frac{1}{k_{eo} - k_{ep} \cdot \dfrac{Z(j)}{\eta f(r_j)}} \right] - \left[\frac{1}{k_{eo} - k_{ep} \cdot \dfrac{Z(i)}{\eta f(r_i)}} \right] \right\} \sqrt{I} \tag{4}$$

where k_{eo} and k_{ep} are constants, the Z are the average valencies, η is the viscosity of the running buffer and the f(r) are a function of the hydrodynamic radius (r) traditionally believed $= r$. (However, recent evidence indicates f(r) $= r^2$ [5]). At fixed temperature (and over a limited range of buffer compositions), η will be approximately constant, and, provided the degree of dissociation of the

analyte (α) is not altered, $Z(j)$ and $Z(i)$ will also remain constant. Assuming also that the r and f(r) are unaltered, Eq. (4) reduces to its simplest form (Eq. (5)):

$$\Delta t_{\text{app}} = (b_j - b_i)\sqrt{I} \qquad (5)$$

where b_j and b_i will also be constants.

3. Experimental

3.1. Instrumental

A Model 270A CE System by Applied Biosystems (Foster City, CA, USA) was used for all CZE experiments. The analytes were detected by UV–Vis absorbance at 254 nm and the detector time constant was set at 0.3 s in all experiments.

Separations were performed at 30°C on a 67.3 cm×50 μm I.D.×220 μm O.D. fused-silica capillary (Applied Biosystems) with the detection window located 49.0 cm from the injection end. Vacuum injection took place at the anode (+).

A Cary 13E UV–Vis spectrophotometer by Varian (Mulgrave, Australia) was used for determination of degrees of dissociation of sulphadiazine and sulphadimethoxine. The analytes were detected at their wavelengths of maximum UV absorbance between 250 and 280 nm.

3.2. Chemicals and materials

The 23 SFAs [sulphanilamide (SAA), sulphaguanidine (SGW), sulphapyridine (SPYR), sulphamethazine (SMZ), sulphisomidine (SISM), sulphamoxole (SMO), sulphamethoxypyridazine (SMOP), sulphathiazole (ST), sulphamerazine (SMR), sulphameter (SME), sulphadimethoxine (SDIM), sulphadiazine (SDI), sulphaquinoxaline (SQ), sulphachloropyridazine (SCP), sulphabenzamide (SBE), sulphamethoxazole (SMOZ), sulphisoxazole (SIOX), sulphamethizole (SMI), sulphacetamide (SAC), phthalyl sulphathiazole (PST), succinyl sulphathiazole (SST), phthalyl sulphacetamide (PSAC) and sulphanilic acid (SA)] used in the study were obtained from Sigma (St. Louis, MO, USA). The structures of the above compounds are shown in Fig. 1.

For the CZE experiments, standard stock solutions of each compound were prepared by precisely dissolving 0.1 g in 100 ml of HPLC grade methanol (BDH). Each compound was diluted with Milli-Q water to give a final concentration of 25 ng/μl. Sample solutions were filtered (0.45 μm) before injection. The sodium phosphate buffers were 65, 101, 174 and 210 mM with respect to phosphate and were prepared from Na_2HPO_4 and NaH_2PO_4 by calculation of the exact amounts required. Precise masses were then dissolved, the solutions magnetically stirred and the stable pH recorded. Where the pH was slightly outside of the range of 7.00±0.05, a small number of drops of 20% H_3PO_4 or 0.1 M NaOH were added to obtain the desired pH of 7.0. Chemicals were of analytical-reagent grade. Buffers for the partition experiments at alternative pH values were prepared in a similar fashion. Organic extractions were performed with mixtures of ethyl acetate and chloroform in the volume ratio of 1:1.

3.3. Methods

3.3.1. CZE

Capillary preparation at the start of each day of experimentation involved initial purging with 0.1 M NaOH for 3 min, followed by Milli-Q water purging for 3 min and then the running buffer for 3 min. Between runs, the capillary was purged with 0.1 M NaOH for 3 min followed by running buffer for 3 min. Vacuum injections of 7 s duration were used. At the nominal 4 nl/s [13], 28 nl would have been injected. However, the more viscous buffers used would lead to greatly reduced injection volumes. Furthermore, as the sample was dissolved in water, sample stacking compensated for this larger than usual volume. All electropherograms were run at pH 7 and 18 kV.

The methanol in the sample solvent acted as a neutral marker (NM) by causing a baseline disturbance in the electropherograms and providing a measure of t_{NM}. The electrophoretic mobility (μ_{ep}) was calculated as usual:

$$\mu_{\text{ep}} = \frac{L_{\text{D}}L}{V}\left(\frac{1}{t_{\text{NM}}} - \frac{1}{t_{\text{app}}}\right)$$

Peak tracking was done using an established method [10].

3.4. Determination of partition constants and degrees of ionisation

These procedures have previously been described in the Theory and Experimental sections of Part II of this series of papers [6]. The exception was for SDIM, where, because the partition constant was so large, measurement in only one phase and calcula-
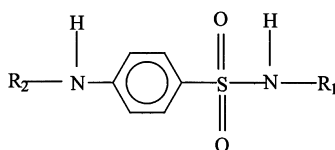
tion by difference was excessively error prone. Hence the concentration of SDIM in the aqueous buffer was also determined by direct measurement.

4. Results and discussion

4.1. The effect of buffer composition

It has been reported that the optimum pH for the separation of 22 SFAs in phosphate buffers is 7 [2].

General structure:

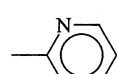Fig. 1. Structural formulas and pK_a values for the 23 sulphonamides.
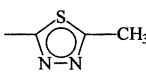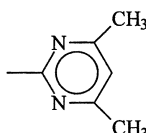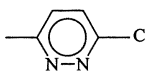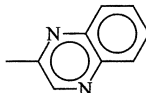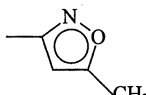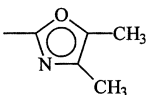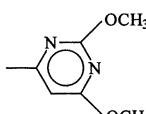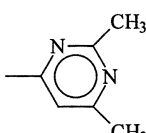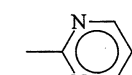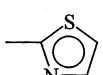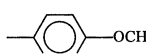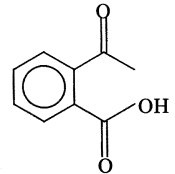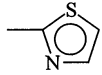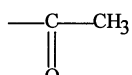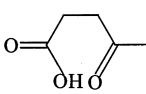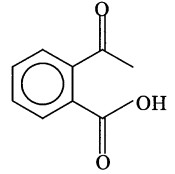
	R_1	$pK_{a,1}$	$pK_{a,2}$		R_1	$pK_{a,1}$	$pK_{a,2}$
SMI (19)			5.4	SMZ (5)		2.4	7.4
SCP (15)			5.5	SPYR (4)		2.6	8.4
SQ (14)			5.5	SAA (2)	H	2.4	10.4
SMOZ (17)			5.6	SMO (7)			
SDIM (13)			6.2	SISM (6)			
SDI (12)		2.0	6.5	PST (21)			
SMOP (8)			6.7	R_2:			
SST (22)				PSAC (23)			
R_2				R_2			

Fig. 1. *(continued)*

The phosphate concentrations used in that study were 30, 50 and 100 mM and it is clear from that data that there are four potentially difficult regions in the separation. Three of these regions can be seen in Fig. 2a. (i) The broad bump at the start of the electropherogram includes the neutral marker [NM (1)], SAA (2) and SGW (3). As the p$K_{a,2}$ values for these two SFA are 10.4 and 11.3, respectively, the electrophoretic mobilities should be negligible at pH 7 and there is little that can be done in CZE to effect separation of this pair from the NM and each other. (ii) The second area of concern comprises SDI (12) and SDIM (13). From the previous study [2], at 30 mM phosphate the resolution of this pair was minimal (R_s estimated to be around 0.55 [11]), at 50 mM the peaks are largely resolved ($R_s \approx 1.1$), but at 100 mM there is no discernable separation. Optimum separation was indicated part way from 50 mM to 100 mM. (iii) The third group requiring improved separation is compounds 15–19. In particular, SBE (16) and SMOZ (17) formed a single band at both 30 and 50 mM but were largely resolved at 100 mM ($R_s \approx 1.1$) [2]. Within this group of five compounds, the other pairs had R_s 0.8–1.0 at 30 mM but were baseline-resolved at 50 and 100 mM. (iv) The final potentially difficult region of the electropherogram involved SAC (20) and PST (21). The t_{app} versus buffer concentration plots for these two compounds crossed over between 70 and 75 mM phosphate.

For factors (ii), (iii) and (iv), respectively, the optimal phosphate concentrations indicated were around 50 mM, towards 100 mM and around 50 or 100 mM but not in the vicinity of 70–75 mM. Hence the first electropherogram was run in 65 mM sodium phosphate (at pH 7 and 18 kV). Fig. 2 shows the critical first two-thirds of the electropherograms obtained for each concentration examined. The last three peaks of the electropherograms [SST (22), SAC (23) and SA (24)] have not been shown since these compounds are well resolved under all conditions, but elute many minutes later and their inclusion would cause compression and loss of detail in the rest of the electropherogram.

The 65 mM run (Fig. 2a) shows distinct peaks for compounds 4–21. With SST (22), PSAC (23) and SA (24) also separated, all of the ionised compounds are sufficiently resolved to allow qualitative analysis (given appropriate internal markers to standardise

any drift in the apparent migration times). The resolution of SDI (12) and SDIM (13) is the same as in the previous study [2] at 50 mM ($R_s \approx 1.1$). It was expected that this would be significantly improved. That this was not observed is probably due to the difference in the buffer (mixed Na$_2$HPO$_4$ and KH$_2$PO$_4$ in the previous study [2]). Support for this explanation is indicated by clear selectivity differences elsewhere. For example, in the previous study [2], for the band of compounds 15–19, it was 16 and 17 that formed one fused peak and the other combinations were all well separated. Fig. 2a shows the opposite of these to be so in 65 mM sodium phosphate. Also, in the previous study PST (compound 21) emerges before SAC (compound 20) in 50 mM buffer but after it in 100 mM buffer, with an inversion implied between 70 and 75 mM phosphate. However, Fig. 2 shows that the migration behaviour in pure sodium phosphate buffer is far simpler. SAC (20) emerges before PST (21) with approximately the same relativity at all buffer concentrations.

The importance of the above difference in buffer composition is significant in that buffer selection may often not be considered as carefully as is deserved. The effect of the buffer cation has been clearly demonstrated by Issaq et al. [12] and the size of the effects of cation substitution in this study (relative to our previous investigation [2]) are compatible with those previously observed [12].

4.2. Systematic effects of the increasing buffer concentration

There are several effects that result directly from increases in the buffer concentration. Two of these are systematic and therefore affect all analytes.

4.2.1. Ionic strength

The first of these systematic effects is a specific example of the more general phenomenon implicit in Eqs. (2)–(5) and explained many years ago by Jorgenson and Lukacs [13]. The smaller the μ_{eo}, the larger the relative effect of differences in μ_{ep} and the greater the separation (Δt_{app}).

One specific example of the above general phenomenon is increasing buffer concentration. Given the previous observations of increased separation with increased ionic strength, to facilitate the sepa-
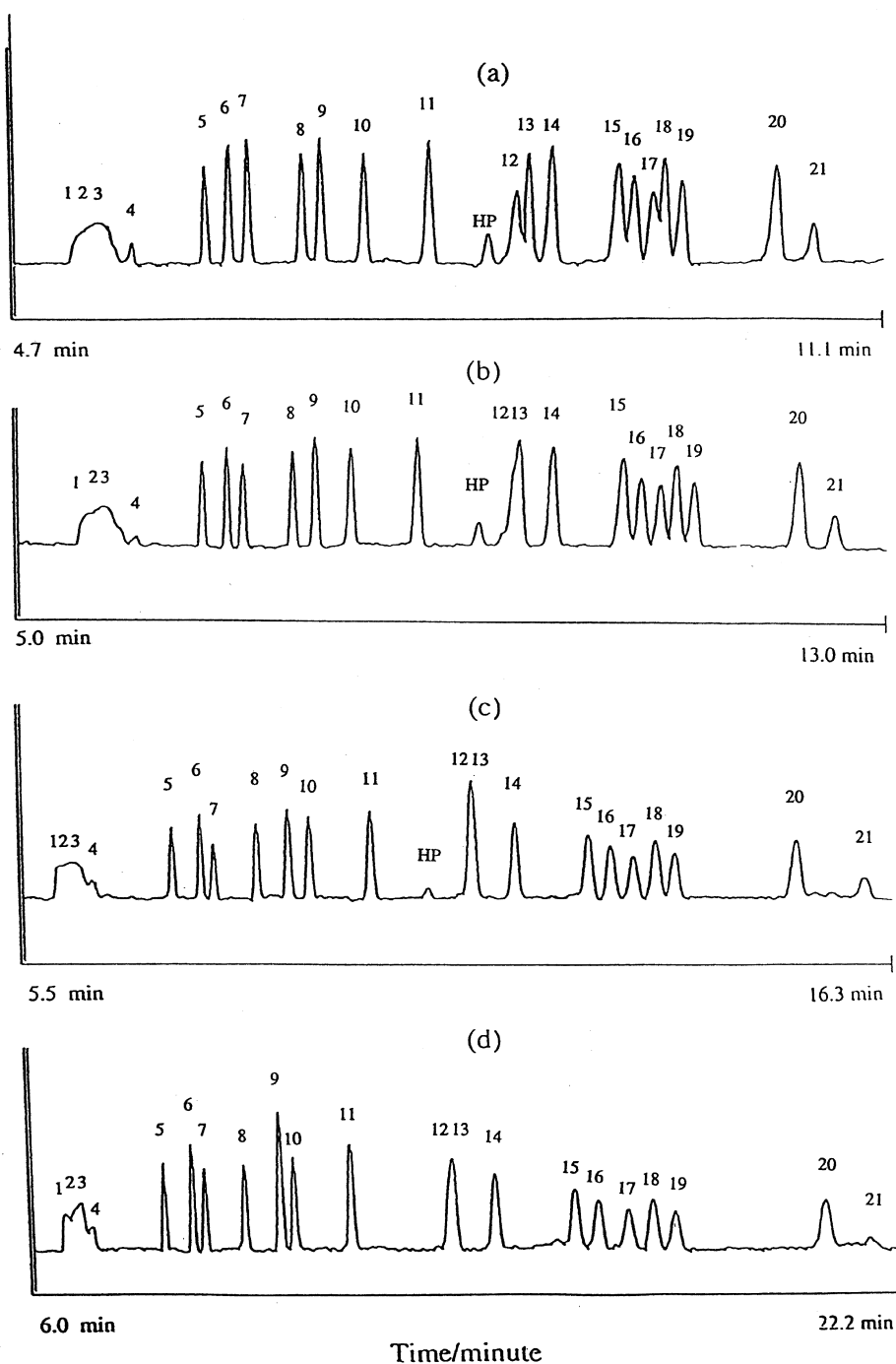
Fig. 2. Electropherograms of the SFAs in sodium phosphate buffers with 18 kV applied at pH 7, (a) in 65 m*M*, (b) in 101 m*M*, (c) in 174 m*M*, (d) in 210 m*M*. Legend: (1) Neutral marker, (2) SAA, (3) SGW, (4) SPYR, (5) SMZ, (6) SISM, (7) SMO, (8) SMOP, (9) ST, (10) SMR, (11) SME, (HP) Hydrolysis product of SMO, (12) SDI, (13) SDIM, (14) SQ, (15) SCP, (16) SBE, (17) SMOZ, (18) SIOX, (19) SMI, (20) SAC, (21) PST, (22) SST, (23) PSAC, (24) SA.

ration, we investigated the effect of higher buffer concentration in the range of 100–210 mM. Fig. 2 shows the results. In general, the expected increases in separation are observed. This is most clearly demonstrated by the group of compounds 15–19 and is particularly obvious when it is realised that between Fig. 2a and Fig. 2d the time scale has been compressed by approximately a factor of three. Thus, on the time scale of Fig. 2a, compounds 15–19 would be separated by three-times the distances indicated in Fig. 2d.

As stated in previous sections, in dilute buffer solutions there is considerable evidence to support the relationship of $\mu_{ep} \propto 1/\sqrt{I}$ [3–6,9]. Under these conditions all of Eqs. (3)–(5) are equally valid but Eq. (5) is much more specific. The $(b_j - b_i)$ term contains the intrinsic differences in charge and size between the two analytes and is the basis for separation, while the $\sqrt{I}$ factor scales the degree of separation: $\Delta t_{app} \propto \sqrt{I}$. However, at higher buffer concentrations where secondary effects begin to operate, Eq. (5) is no longer valid and plots of t_{app} versus $\sqrt{I}$ cease to be linear [6,7].

4.2.2. Joule heating

Fig. 3 shows the effect of the square root of ionic strength upon the apparent migration times (at pH 7 with 18 kV applied). In qualitative agreement with the theory, the migration times of the solutes have clearly spread with increasing ionic strength. However, the dependence is not linear, there being an increasing rate of curvature towards higher $\sqrt{I}$. These systematic increases in curvature of the plots in Fig. 3 have been demonstrated to be due to the onset of Joule heating [6]. Under these circumstances, Eq. (5) is inadequate and Eq. (4) is required to explain the observed behaviour. However, this can only be done with the aid of the specific behaviour of μ_{eo} and μ_{ep} as a function of $1/\sqrt{I}$. Fig. 4 shows these data. The exact concentrations of phosphate investigated were 65 mM ($1/\sqrt{I} = 2.95$), 101 mM ($1/\sqrt{I} = 2.36$), 174 mM ($1/\sqrt{I} = 1.81$) and 210 mM ($1/\sqrt{I} = 1.65$). Thus the effect of increasing buffer concentration can be seen from right to left in Fig. 4.

In the case of μ_{eo}, there is a decrease that appears approximately linear until the highest buffer concentrations (lowest $1/\sqrt{I}$). This behaviour is consistent with that observed by Salomon et al. [14] in their study of electroosmosis in concentrated NaOH solutions ($1/\sqrt{I} = 0.2$–0.8). In that case the EOF increased rapidly and linearly from below $1/\sqrt{I} = 0.2$ up to about 0.4 where the plot curved over and began to exhibit the transition from high buffer concentration behaviour towards the linear low buffer concentration behaviour observed by Janini et al. [3] at $1/\sqrt{I} = 3.65$ and above. Our data falls between these two sets of data and is qualitatively consistent with both of them. In particular, as μ_{eo} is expected to be proportional to $1/\sqrt{I}$ in dilute buffers, the values measured at lower buffer concentrations are as expected.

In the case of the μ_{ep}, the situation is more complex. In part II of this series of papers [6] we demonstrated that μ_{ep} approaches linearity around $1/\sqrt{I} = 6$–8 (at the applied voltage used in this study). Hence at ionic strengths lower than in Fig. 4 ($1/\sqrt{I}$ higher), the plots of μ_{ep} would bend over and approach linearity with a negative gradient. Extrapolating these linear segments back to the range of $1/\sqrt{I}$ in Fig. 4 would show that the measured μ_{ep} in Fig. 4 lie well below the extrapolated dilute solution behaviour. These increases in the magnitudes of the μ_{ep} values of the SFAs are principally due to Joule heating and decreased η [6].

Returning to Eq. (4), it must be remembered that the quasi constant k_{eo} term contains all of the quantities that make up μ_{eo} other than $1/\sqrt{I}$. One of the quantities in the numerator of k_{eo} and μ_{eo} is η. Therefore it would be possible to take η from all of the terms in the differences in the denominators in Eq. (4) and place it as a multiplier alongside the $\sqrt{I}$. This would be in accord with the accepted identical dependences of μ_{eo} and μ_{ep} upon η but would predict decreases in t_{app} and Δt_{app} due to decreasing η (relative to the extrapolated dilute solution behaviour). That is, the plots of t_{app} in Fig. 3 would be predicted to curve down and the separations decrease; the opposite of that observed.

From Fig. 4, it appears that k_{eo} does remain approximately constant over the range of buffer concentrations examined as μ_{eo} is approximately linear with respect to $1/\sqrt{I}$. This implies that another factor in k_{eo} changes with increasing temperature and I and largely compensates for the decreasing η. (A change in the rate of alteration of the silica surface
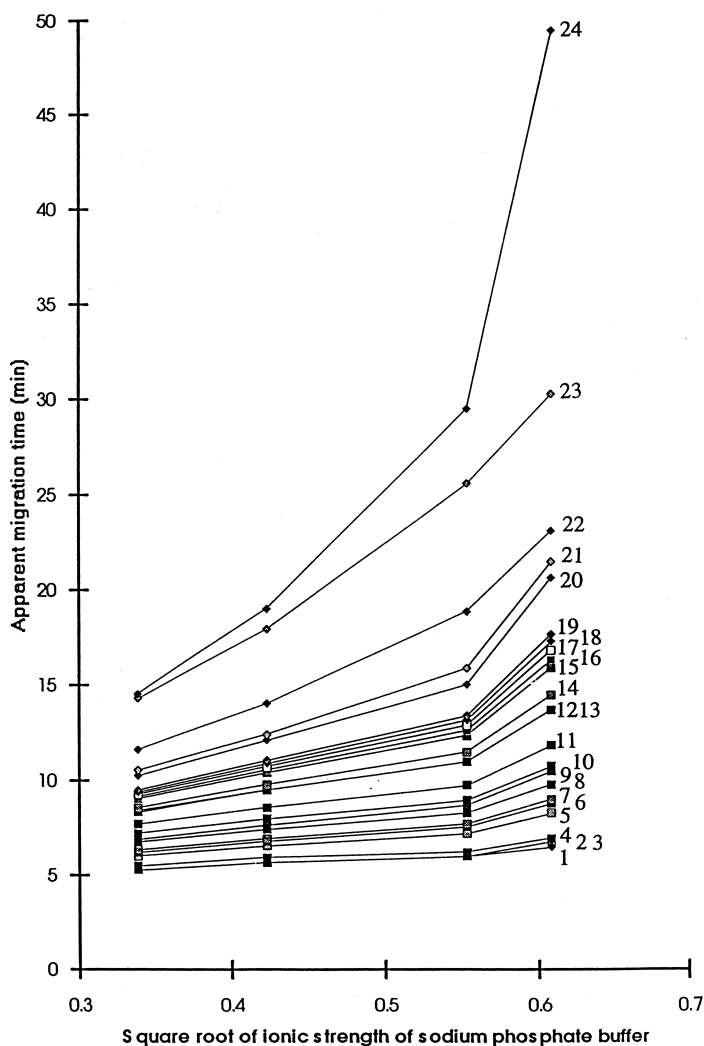
Fig. 3. Apparent migration times of the 23 SFAs versus the square root of ionic strength of the sodium phosphate buffer (18 kV applied at pH 7). Legend for the compounds as in Fig. 2.

excess charge density suggests itself). This being the case, η effectively increases only μ_{ep} (and not μ_{eo}) over most of the range of I examined. It is clear that care is required in the manipulation and interpretation of Eq. (3).

Thus the systematic decreases in apparent mobilities of the analytes and the increases observed in t_{app} and Δt_{app} in Fig. 3 may be attributed to a combination of three effects. At low ionic strengths (well below $\sqrt{I}=0.3$) there is a linear dependence of t_{app} and Δt_{app} upon $\sqrt{I}$ which arises from the salt

effects upon μ_{eo} and μ_{ep}. These are the two effects demonstrated by Janini et al. [3]. In the region of our experimentation (above $\sqrt{I}=0.3$, Fig. 3) there is the additional effect of Joule heating, which – as explained above – appears to only effect μ_{ep}. As our previous study [6] indicates a non-linear increase in Joule heating with buffer concentration (at least at high concentrations), the increasing curvature of the plots in Fig. 3 are to be expected. With temperature rises indicated [6] at about 2, 3, 5 and 7°C for the 65 mM ($\sqrt{I}=0.339$, $1/\sqrt{I}=2.95$), 101 mM ($\sqrt{I}=0.423$,
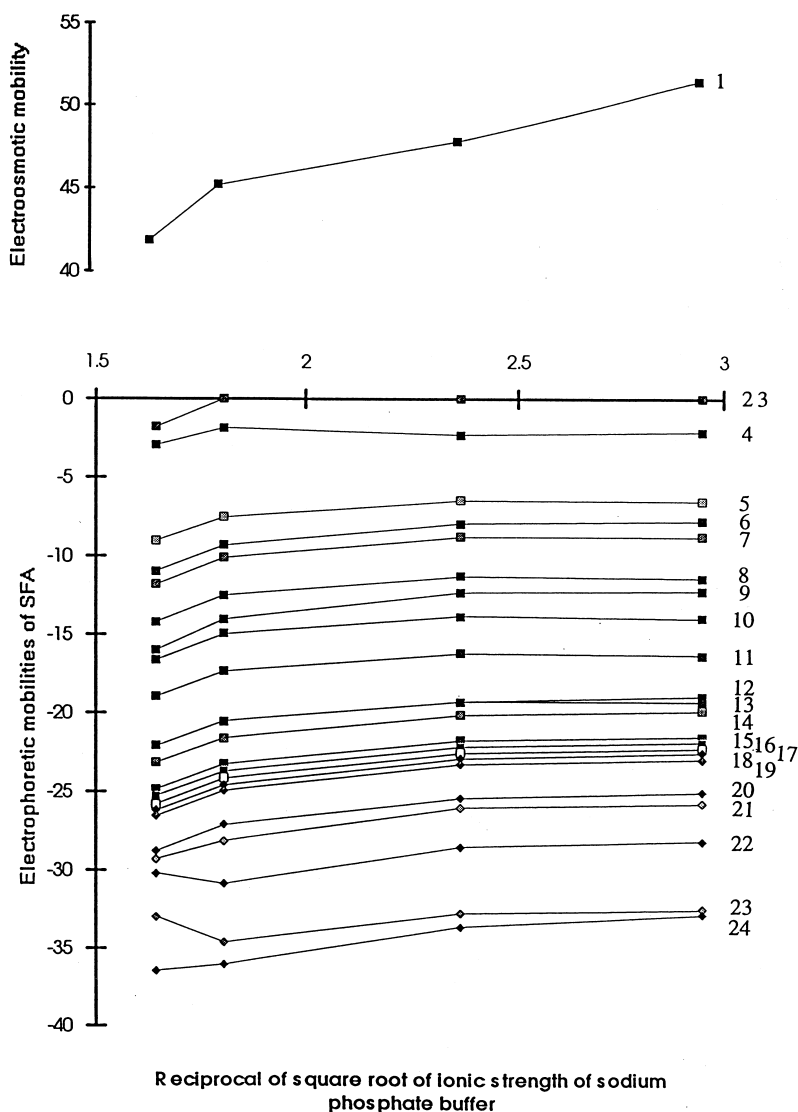
Fig. 4. Electroosmotic mobility and the electrophoretic mobilities of the 23 SFAs (cm^2 10^{-5}/V s) versus the reciprocal of the square root of ionic strength of the sodium phosphate buffer. Legend for the compounds as in Fig. 2.

$1/\sqrt{I}=2.36$), 174 mM ($\sqrt{I}=0.553$, $1/\sqrt{I}=1.81$) and 210 mM ($\sqrt{I}=0.606$, $1/\sqrt{I}=1.65$) buffers and 18 kV, respectively, using the rule of thumb of 2.4% increase in mobilities per °C [14], the changes in μ_{ep} are around 5, 7, 12 and 17%. These modest changes are compatible with the changes in μ_{ep} observed in Fig. 4, but are highly magnified in t_{app} (Fig. 3) where they are superimposed on decreasing μ_{eo} and give rise to the rapid upturn in apparent migration times.

This magnification may have been further emphasised by the accelerated rate of decrease of μ_{eo}, as is indicated at the high end of the buffer concentration range (Fig. 4).

4.3. Selective effects of increasing buffer concentration

As the relativities of the μ_{ep} values change for

analytes 12 (SDI) and 13 (SDIM) (Fig. 4), the question that arises is whether it is the leading compound that is retarded by the presence of higher concentrations of buffer, or whether it is the following compound that is accelerated.

Differential changes in ionisation are the obvious source of selectivity variations in CZE and around pH 7 the SFAs are controlled by $pK_{a,2}$; the electrically neutral acid conjugate being in equilibrium with the deprotonated (sulphon)amide anion. Since the overall salt effect on ionisation is very difficult to predict [6], both in magnitude and direction, we have measured the effects for SDI and SDIM.

4.3.1. Isothermal salt effects upon ionisation

Fig. 5 shows the salt effects upon the ionisation of SDI and SDIM at 30, 35 and 40°C. For both of the analytes, and at all of the buffer concentrations examined, the degree of ionisation (α) increases with temperature. We have also found this to be the case in our previous study [6] (SMZ and ST) and in a more extended examination of ionisation [15] (SMZ,
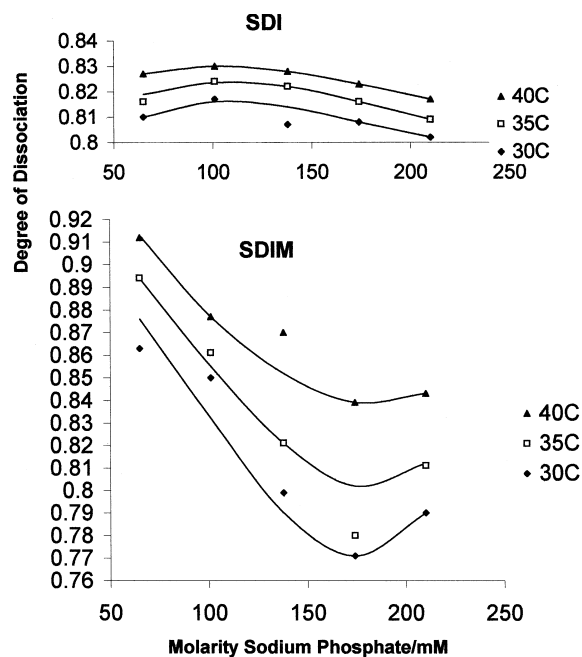
ST, SISM, SMO, SMOP, SME, SMR, SDI and SDIM). In all cases, in each of the three studies, increasing buffer (sodium phosphate, pH 7) concentration causes a systematic change in α and can therefore potentially give rise to changes in selectivity. The manner in which α varies with buffer concentration (at fixed operating temperature) is highly variable [6,15] and is frequently subject to reversals in direction, as is the case for both SDI and SDIM. Given that there are both salt and thermal effects due to Joule heating, this is not too surprising. The way in which the variation of α with buffer concentration increases with temperature is also sometimes complex, although for SDI and SDIM (Fig. 5) this is not the case. And finally, the basic issue of increased or decreased ionisation with increasing buffer concentration does not correlate simply with any of $pK_{a,2}$, structure or size. Some closely related compounds do exhibit very similar behaviour, but others that are not apparently different in any significant way display quite different behaviour. For example, from Fig. 1 it can be seen that SME and SMOP are virtually identical in $pK_{a,2}$, structure and size and they show remarkably similar variations in ionisation as a function of both buffer concentration and temperature [15]. By contrast, given the similar migration times, SMZ and SISM are equally closely related. However, the salt effects on ionisation are the opposite [15].

From Fig. 1 it can be seen that SDI and SDIM have similar structures and $pK_{a,2}$ values, whilst the salt effects are quite different. The molecular differences are the positioning of the nitrogen atoms in the heterocycle and the two weakly polar additional methoxy groups that makes SDIM slightly larger. In this instance, the general rules for salting in and salting out seem to adequately explain the relative differences in the isothermal salt effects upon ionisation. The electrically neutral SDI molecule is smaller (than SDIM) and on average would be slightly more polar. Hence it would not be expected to be strongly salted out (and might be salted in). As the observed net salt effect upon ionisation is only small for SDI (Fig. 5), significant salting in of the acid conjugate is implied; sufficient to neutralise the salting in of the basic conjugate. On the other hand, being larger and slightly less polar, the SDIM acid conjugate would be expected to be less stabilised by increasing buffer

Fig. 5. Isothermal salt effects upon ionisation. The degree of dissociation (α) for SDI and SDIM versus the sodium phosphate buffer concentration for temperatures in the region of experimentation.

concentration. The plots in Fig. 5 for SDIM indicate this to be so since they are similar in shape to the typical activity coefficient curves expected for ions (the basic conjugate) and imply only a small salt effect on the electrically neutral conjugate.

The ionisation data in Fig. 5 indicates opposing salt effects on SDI and SDIM. At the low end of the buffer concentration range, the more mobile, later emerging SDIM (compound 13 in Fig. 4) experiences decreased ionisation and mobility as the buffer concentration increases. The less mobile, earlier emerging SDI (compound 12 in Fig. 4) becomes slightly more ionised and mobile and the electrophoretic mobilities of the two compounds can be seen to converge in the 101 mM buffer (Fig. 4, $1/\sqrt{I} = 2.36$). From the data in Fig. 5, differing rates of change of ionisation extend beyond 101 mM buffer and inspection of the electropherograms in Fig. 2 clearly indicate that SDI (12) and SDIM (13) do not exactly comigrate until towards 174 mM buffer. In this vicinity, both analytes experience decreasing ionisation for some time and continue to comigrate. The foregoing correlation of isothermal ionisation behaviour with electrophoretic mobility variation as buffer concentration changes is, however, only a first approximation. Ionisation of the analytes will concurrently be altered by salt and thermal effects.

4.3.2. Combined thermal and salt effects upon ionisation

Fig. 6 displays the same ionisation data as Fig. 5, but in this case α is plotted versus temperature for each buffer concentration. And for each of these buffer concentrations we have indicated the temperatures arising from Joule heating (large circles), as previously determined [6]. When these points are joined together (heavy curves), the resultant changes in ionisation are those due to the combined effects. Although not quantitatively exact, the match between the net variations in the ionisation behaviour and the electrophoretic mobilities is good, with the exception of the upturn in ionisation for SDIM at the highest buffer concentrations.

4.3.3. Adsorption

For SDI and SDIM, the above analysis of electrophoretic behaviour appears to be close to complete.
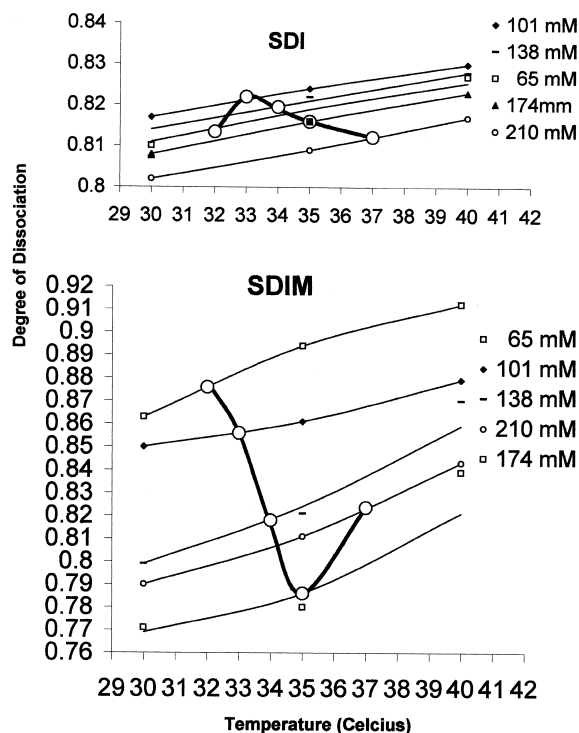

Fig. 6. Combined thermal and salt effects upon ionisation. The degree of dissociation (α) for SDI and SDIM versus temperature for the various experimental sodium phosphate buffer concentrations (finer curves). The large circles on these finer lines indicate the average internal capillary temperature at each buffer concentration and the solid curves show the variation in α when both ionic strength and Joule heating are taken into account.

However, that may not be the case for all analytes, or indeed all SFAs.

Firstly, in a broader (preliminary) study of the salt effects upon the ionisation of the SFAs [15] it was found that the size of salt effects upon ionisation for the SFAs is highly variable. For example, partition measurements indicate the combined salt and temperature effects for SMOP in sodium phosphate buffers at pH 7 are $\alpha = 0.378$ at 101 mM buffer, 0.532 in 138 mM, 0.633 at 174 mM and 0.560 at 210 mM buffer. As this appears to be the extreme case, the 67% increase in ionisation between 101 and 174 mM buffer would be expected to manifest itself in a huge and obvious increase in μ_{ep}. Inspection of Fig. 4 in this paper shows this not to be the case. In fact curve 8 (SMOP) is remarkably similar to most of the other curves. Some other factor countering the

increased ionisation is inferred. For this particular analyte, this is not surprising. In studies of other aspects of the electrophoretic behaviour [5,16], SMOP has usually been a clear outlier relative to the large group of the SFAs that we have used as target analytes.

Secondly, in part II of this series [6], it was also notable that one of the SFA probes used (ST) yielded strongly discordant estimates of Joule heating. As these estimates were based upon electrophoretic behaviour corrected for ionisation, again there is evidence for another determinant of net mobility of ions in CZE.

The third piece of evidence for another selective factor in the determination of electrophoretic mobilities is provided by SAA (2) and SGW (3). The broad band at the start of the electropherograms in Fig. 2 clearly indicates that these two analytes either have some finite electrophoretic mobility or alternatively are retarded by some other mechanism. By 210 mM phosphate there is partial resolution from the neutral marker (Fig. 2d). As the p$K_{a,2}$ values are 10.4 and 11.3, it does not seem conceivable that the electrophoretic mobilities could be other than negligible at pH 7, even for an order of magnitude shift in the ionisation.

The only mechanism that appears to be available is adsorption. Contact adsorption of the negatively charged SFA on the negatively charged silica surface seems highly unlikely. However, with the SFA negative charge centred in the molecule, hydrogen bonding between the protons of the primary amine at one end with dissociated silanol anions does not seem impossible. Such interactions are well known to reversed-phase liquid chromatographers through the tailing of amine-containing analytes. Also, the SFA will be in dynamic equilibrium with their conjugate acids which are uncharged and comprise a significant percentage of the analytes. Whilst the approach of the anionic SFA towards the anionic silica surface will be inhibited by the Donnan potential, the excess charge on the solution side of the electrical double layer is just that; excess charge and not the total charge. Anions are electrostatically adsorbed so the anionic SFA could spend some time stationary between the slipping plane and the inter-

face, either in the inner part of the diffuse region of the double layer or in the outer part of the compact region. This could result in a small but significant amount of retention in the vicinity of the capillary walls. If this retention is a normal part of the electrophoretic process, then there will be a distribution of the extent of adsorption about the average amount for any group of molecules. Thus changes in ionisation due to salt and Joule heating effects may be modified, whether ionisation is enhanced or suppressed.

Acknowledgements

References

[1] R.F. Cross, J. Chromatogr. 478 (1989) 422–428.
[2] M.C. Ricci, R.F. Cross, J. Microcol Sep. 5 (1993) 207–215.
[3] H.J. Issaq, I.Z. Atamna, G.M. Muschik, G.M. Janini, Chromatographia 32 (1991) 155–161.
[4] R.J. Wieme, in: E. Heftmann (Ed.), Chromatography, A Laboratory Handbook of Chromatographic and Electrophoretic Methods, Van Nostrand Reinhold, New York, 3rd ed., 1975, Ch. 10.
[5] R.F. Cross, J. Cao, J. Chromatogr. A 786 (1997) 171–180.
[6] R.F. Cross, J. Cao, J. Chromatogr. A 809 (1998) 159–171.
[7] J. Cao, R.F. Cross, J. Chromatogr. A 695 (1995) 297–308.
[8] R.F. Cross, J. Cao, Proceedings of the Royal Australian Chemical Institute 13th Symposium on Analytical Chemistry, Darwin, July 1995, RACI Analytical Chemistry Division, pp. AO18/1-4.
[9] T. Tsuda, K. Nomura, G. Nakagawa, J. Chromatogr. 248 (1982) 241–247.
[10] R.F. Cross, LC·GC 7 (1989) 418–423.
[11] L.R. Snyder, J.J. Kirkland, in: Introduction to Liquid Chromatography, Wiley, New York, 2nd ed., 1979, Section 2.5.
[12] I.Z. Atamna, C.J. Metral, G.M. Muschik, H.J. Issaq, J. Liq. Chromatogr. 13 (1990) 2517–2527.
[13] J.W. Jorgenson, K.D. Lukacs, Anal. Chem. 53 (1981) 1298–1302.
[14] K. Salomon, D.S. Burgi, J.C. Helmer, J. Chromatogr. 559 (1991) 69–80.
[15] J. Cao, R.F. Cross, unpublished data.
[16] R.F. Cross, M.C. Ricci, LC·GC 13 (1995) 132–142.